
Platonic Grounding for Efficient Multimodal Language Models

Moulik Choraria^{1*} Xinbo Wu^{1*} Akhil Bhimaraju¹ Nitesh Sekhar² Yue Wu² Xu Zhang² Prateek Singhal
Lav R. Varshney¹

Abstract

The hyperscaling of data and parameter count in Transformer-based models is yielding diminishing performance improvement, especially when weighed against training costs. Such plateauing indicates the importance of methods for more efficient finetuning and inference, while retaining similar performance. This is especially relevant for multimodal learning paradigms, where inference costs of processing multimodal tokens can determine the model’s practical viability. At the same time, research on representations and mechanistic interpretability has improved our understanding of the inner workings of Transformer-based models; one such line of work reveals an implicit alignment in the deeper layers of pretrained models, across modalities. Taking inspiration from this, we motivate and propose a simple modification to existing multimodal frameworks that rely on aligning pretrained models. We demonstrate that our approach maintains and, in some cases, even improves performance of baseline methods while achieving significant gains in both training and inference-time compute. Our work also has implications for combining pretrained models into larger systems efficiently.

1. Introduction

Although scaling has proven effective in training powerful Transformer-based models (Kaplan et al., 2020; Zhai et al., 2021; Hoffmann et al., 2022), growing awareness of the enormous costs of large models (Strubell et al., 2019; Grattafiori et al., 2024) has shifted the focus to efficient finetuning of pretrained models and speeding up their inference (Hu et al., 2021a; Leviathan et al., 2023). Similarly, for multimodal applications such as vision-language understanding, starting with pretrained unimodal models reduces the training burden compared to initialization from scratch

(Qi et al., 2024). Even so, efficiency gains remain desirable due to the added burden of processing multimodal tokens alongside natural language prompts.

Within multimodal applications, vision-language models (VLMs) are a prominent area of research (Radford et al., 2021; Li et al., 2022; Liu et al., 2024b). Advances in large language models (LLMs) (Brown et al., 2020; Chung et al., 2022; Touvron et al., 2023; OpenAI et al., 2024) have spurred the development of general-purpose VLMs capable of harnessing multimodal inputs for simultaneous visual and textual comprehension across diverse applications and domains. The key to effective VLM training is cross-modal alignment. This is usually achieved via multi-stage training: a pretraining stage with image-text pairs, followed by instruction finetuning for specialized vision downstream tasks (Dai et al., 2023). Preference tuning techniques, such as reinforcement learning from human feedback (RLHF) (Ouyang et al., 2022) can yield further improvements for this alignment (Sun et al., 2023b; Wang et al., 2024). However, most works on improving cross-modal alignment propose modifications to the training algorithm and/or choice of dataset, while largely treating the pretrained components as replaceable black box models.

Motivating our framework are the following two key observations. First, it was recently shown that model representations across vision and language show increasing alignment in the deeper layers (see Fig. 2 and Huh et al. (2024)). Second, analyzing the vision to language attention in pretrained VLMs reveals that the bulk of the activity is confined to the middle and latter layers (see Fig. 3). This raises a natural question: *Which layers are really necessary for multimodal token processing in VLMs and can we find and remove redundancies?* Our key contribution is answering this in the affirmative: **We show that simple architectural modifications can yield similar (and even improved) performance, while offering significant gains in model efficiency.** To that end, we modify the VLM forward pass to process the multimodal tokens in only the latter layers, revealing a natural performance-efficiency tradeoff (see Fig. 1) We refer to this architectural modification framework as Platonic grounding.

Remark. We do not claim any particular relation to the area

¹University of Illinois Urbana-Champaign ²Amazon. Correspondence to: Moulik Choraria <moulikc2@illinois.edu>.

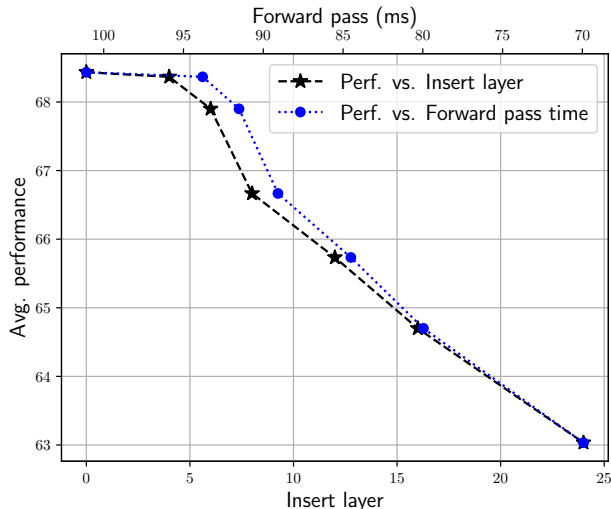


Figure 1. Tradeoff between performance and computational efficiency in LLaVA v1.5-7B. The input prompt consists of an image and a text query asking for a description of that image. The insert layer index i denotes that the visual tokens are directly fed into the $(i + 1)$ th layer, thereby reducing the compute requirements. The latter is more explicitly measured via the decreasing average time per forward pass of the models. However with insertion in the latter layers, efficiency comes at the cost of a degradation in average performance as there are fewer layers available for visual processing. Via Platonic grounding, we aim to find the sweet spot (in this figure, between layers 4-6) that allows for maximum efficiency with minimal degradation.

of “language grounding” in computer vision, concerned with relating objects in larger scenes to their textual descriptions. Rather, we build on quotidian uses of the term “grounding” in several fields such as cognitive science (Barsalou, 2010) and linguistics (Buccino et al., 2016). Our use of the term “Platonic” reflects a connection to the Platonic hypothesis (Huh et al., 2024), which originally motivated us.

This paper is organized as follows. We begin by outlining the scope of our work in the context of broader literature in Sec. 2. Then, Sec. 3 motivates the Platonic grounding framework, based on the analysis of preexisting alignment in modalities as well as the functioning of trained VLMs. Sec. 4 details the general notion, highlighting implementation and design considerations. Experiments in Sec. 5 demonstrate the versatility and effectiveness of grounding across a variety of popular VLMs, in terms of both performance and efficiency. Note that while the bulk of our exposition focuses on VLMs, we also include experiments with multimodal molecular language modelling to demonstrate the more general potential of our approach. We conclude with promising directions for broader application in Sec. 6. In addition to our more practical contributions, our work alludes to novel underlying mechanisms for multimodal

processing, which may be of independent interest.

2. Related Work

Vision-language models: The type of VLMs considered in this work consist of a pretrained autoregressive LLM that consume both text and visual tokens, the latter of which are obtained from a pretrained vision encoder (Radford et al., 2021; Sun et al., 2023a). Additionally, a fusion module (for instance, an MLP in LLaVA, Perceiver in Flamingo or QFormer in BLIP) (Alayrac et al., 2022; Li et al., 2023a; Liu et al., 2024a) is used to transfer the visual tokens to a suitable input representation for the LLM. In this work, we adhere to this general backbone but modify where within the LLM the visual tokens are transplanted.

Alignment: Akin to the idea of convergent realism in philosophy (Locke, 1690; Putnam, 1982) and reminiscent of structural and representational similarities across modalities in mammalian cortex (Mountcastle, 1997; Kriegeskorte & Kievit, 2013), there is an increasing body of literature arguing that well-trained neural networks are converging to similar representations (Lenc & Vedaldi, 2015; Tian et al., 2020; Zimmermann et al., 2022). More specifically, Lenc & Vedaldi (2015) proposed the idea of model stitching, that is, *grafting* initial layers of a neural network onto the latter half of another with an affine layer. The resulting performance can then serve as an indicator for the intrinsic representational alignment. Moschella et al. (2023) further highlighted the possibility of achieving it even without the affine layer, in a zero-shot sense. In that regard, our work can be seen as exploiting multimodal model stitching for efficiency, without any additional bells and whistles.

Efficiency: Low-Rank Adapters (LoRA) are a key approach for efficient finetuning, relying on training only a small set of additive parameters with a low-rank constraint, while keeping the base model fixed (Hu et al., 2021b; Dettmers et al., 2023). This reduces memory requirements during training, but inference remains just as costly. Another alternative is model compression; an existing VLM can be distilled effectively, leading to accelerated inference and almost-at-par capabilities (Fang et al., 2021; Wang et al., 2022). However, these approaches naturally need strong base VLMs. In contrast, our method modifies the base VLM itself, providing a complementary approach for even better efficiency.

3. Motivation

This section motivates our proposed framework. First, since pretrained models serve as key building blocks for VLMs, we explore the nature of representational alignment in prominent pretrained models. Second, by visualizing attention head activations, we qualitatively analyze where, within one

forward pass, visual tokens attend to the language tokens in a next token prediction setting. We base our experiments on the LLaVA model (Liu et al., 2024a), one of the most popular open-source VLM frameworks. The first experiment measures the natural alignment in the unimodal components before any LLaVA training, whereas the second experiment studies the forward pass of a trained LLaVA model.

3.1. Natural Vision-Language Alignment

We begin with some formal exposition to characterize the notion of alignment, borrowed from Huh et al. (2024). A representation is a function $\mathbf{f} : \mathcal{X} \rightarrow \mathbb{R}^n$ that assigns a feature vector to each input in some data domain \mathcal{X} . A kernel, $\mathbf{K} : \mathcal{X} \times \mathcal{X} \rightarrow \mathbb{R}$, characterizes how its corresponding representation measures distance/similarity. It is defined as $\mathbf{K}(x_i, x_j) = \langle \mathbf{f}(x_i), \mathbf{f}(x_j) \rangle$, where $\langle \cdot, \cdot \rangle$ denotes the inner product, $x_i, x_j \in \mathcal{X}$, and $\mathbf{K} \in \mathcal{K}$. Finally, a kernel-alignment metric, $\mathbf{m} : \mathcal{K} \times \mathcal{K} \rightarrow \mathbb{R}$, measures the similarity between two kernels, that is, how similar is the distance measure induced by one representation to the distance measure induced by another. As in Huh et al. (2024), we rely on a mutual nearest-neighbor metric that measures the mean intersection of the k -nearest neighbor sets induced by two kernels (normalized by k).

In essence, we measure the distance between the kernels induced by the representation spaces of language and vision. First, these representations are obtained by passing paired image-caption data through the respective pretrained models. Then, we rely on a mutual k -nearest neighbor alignment metric to estimate the alignment between the corresponding feature spaces. We want to understand how alignment varies as a function of model depth, with the intuition that layers capturing “world semantics” are likely to align better, even across modalities. For the LLaVA v1.5-7b model, its starting components include the vision encoder, clip-vit-large-patch14-336 (Radford et al., 2021), and the decoder-only LLM vicuna-v1.5-7b model (Zheng et al., 2023). To compute the alignment metric, we use $k = 10$ nearest neighbors over 1024 samples from WIT (Wikipedia-based Image Text; (Srinivasan et al., 2021)); additional details can be found in Huh et al. (2024).

The alignment plot in Fig. 2 is in line with our expectations: the penultimate layer of the vision model aligns more with the latter layers of the LLM. This may point to some shared semantics in the deeper layers of the respective models, and can perhaps be exploited in designing alignment frameworks for VLMs.

Remark: Although we use the CLIP-based encoder for this experiment, note that this alignment is more general. Fig. 5 in the Appendix demonstrates a similar trend in DINO-based encoders (Caron et al., 2021). This is remarkable as it points to a more general preexisting alignment, since DINO vision

encoders are—unlike CLIP—trained in a self-supervised language agnostic fashion.

3.2. Where Visual Tokens Matter

A line of literature on mechanistic interpretability suggests that the forward pass in an LLM can be broadly delineated into phases: a) the function determination phase that processes the prompt to determine the task that needs to be executed (for instance, *get_capital()*) and b) the execution of the function for the given input query (*get_capital(France) = Paris*) (Hendel et al., 2023; Merullo et al., 2024; Lv et al., 2024). These observations lead us to ask whether a similar delineation holds for VLMs: if we interpret the multimodal tokens as the input query, can we pinpoint where within the LLM does the bulk of the query execution take place? We do so by using attention maps as a proxy with the intuition that a stronger vision-to-language token interaction is reflected in a larger attention score.

Our approach is as follows. We start with a pretrained LLaVA model. We then feed an image along with a multiple-choice question (following the recommended prompt format) to induce the model to respond with a single token (choices A, B, C, or D) as output. This ensures easier analysis, since a single forward pass captures the relevant attention activity. The corresponding attention scores (averaged across attention heads) for vision-to-language token activation are obtained as a function of model depth. For clarity, we randomly subsample vision tokens (80 out of 576 tokens) and arrange them left to right in order of increasing positional indices. The attention response is averaged over 1000 image-prompt pairs obtained from the COCO-2017 training set, as presented in Fig. 3.

It is evident that aside from the flurry of activity in the first and last layers, vision tokens tend to interact with language tokens predominantly in the intermediate layers. This lends credence to our intuition that vision-to-language information transfer is stronger in intermediate layers and that the earlier layers are somewhat redundant when it comes to performing this effectively. We note that an alternate line of experimentation reveals similar findings (Jiang et al., 2025), albeit with the motivation to study object hallucination.

Remark. In the complete layer-wise depiction in the Appendix (Fig. 6), there is a strong activation pattern in the first two layers that dominates all other activity. However, given the nascent nature of language representations in the early stages, we suspect this interaction is unlikely to be the key point of vision-to-language information transfer. In fact, unlike activation in the middle layers, Basu et al. (2024); Jiang et al. (2025) suggest that this behavior is model-specific (i.e., LLaVA), and is not consistently observed for other choices of VLMs/encoders. Consequently, we do not include the first two layers in Fig. 3 to keep the visualization cleaner.

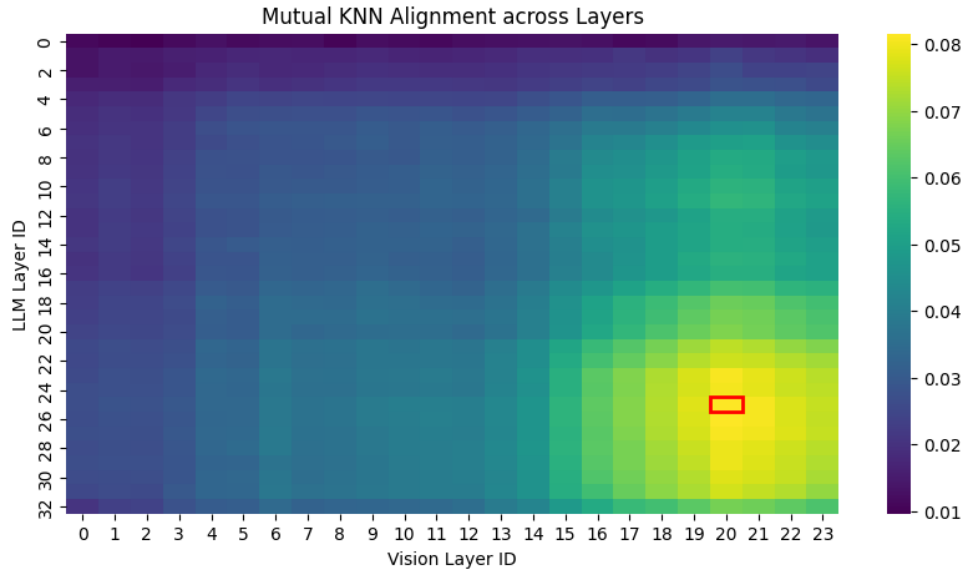


Figure 2. Visualization of intrinsic alignment between pretrained vision (CLIP-based ViT) and language models (Vicuna v1.5), as a function of depth. The vertical axis represents the LLM layer indices, whereas the horizontal axis does the same for the vision encoder. The key point is that for the representations from the latter vision layers (which are generally used as embeddings), alignment becomes stronger as one moves deeper into the LLM.

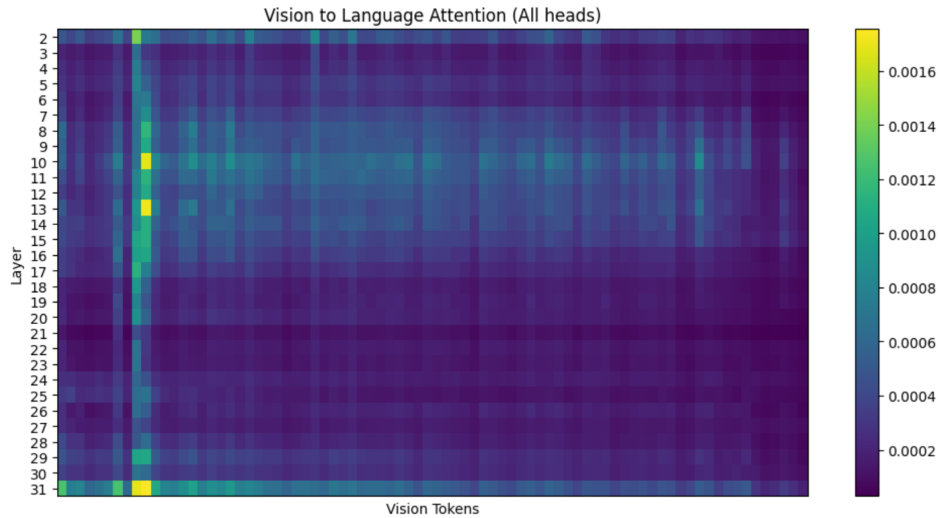


Figure 3. An illustration of vision to language token activations, in the forward pass of a LLaVA-v1.5-7B model. The vertical axis represents the LLM layer indices i.e. depth, whereas the horizontal axis consists of vision tokens in the forward pass, arranged left-to-right in increasing order of positional indices. The legend represents the attention activity averaged across the 32 attention heads in each self-attention layer. The figure suggests that the intermediate layers ($\sim 7-18$) represent the strongest regions of sustained activity for the vision tokens.

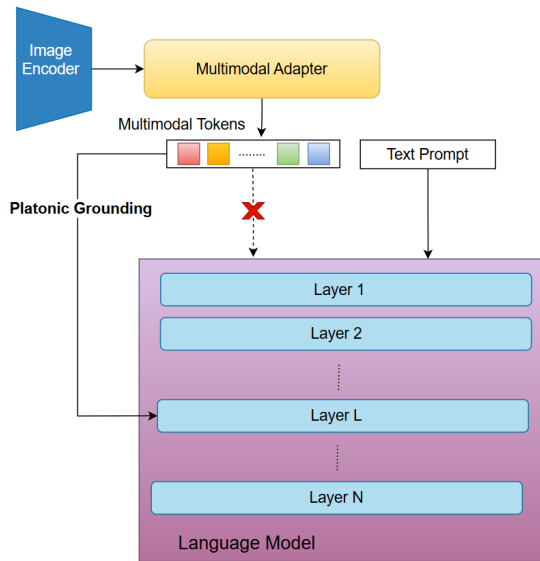


Figure 4. Illustration of Platonic grounding: Instead of feeding multimodal tokens in the first layer along with the text prompt, we bypass the first L layers of the LLM to directly feed them as input to the $(L + 1)$ th intermediate layer, thus reducing the processing requirements for the vision tokens by a fraction of $\frac{L}{N}$.

4. Proposed Framework

Our observations in the previous section indicate that there is both stronger alignment and heavier use of the vision information in the latter layers. This begs the question: *Do we really need all of the LLM layers to parse vision information?* That is, can we use this intrinsic alignment to maintain or potentially even improve performance while limiting multimodal processing to only latter layers?

To investigate, we propose a simple yet effective modification for general VLM frameworks: inserting the vision (more generally, multimodal) tokens directly into the intermediate layers of the LLM. In some sense, we want to directly match semantics in the representation spaces. As it is in line with the Platonic hypothesis, we call it *Platonic grounding*. Fig. 4 illustrates the general approach.

4.1. Technical Challenges

Although fairly straightforward as an abstraction (Fig. 4), our approach has several challenges, some of which are specific to the VLM in question. Recall that whereas vision tokens are inserted in the intermediate layer, language tokens still must be processed by the entire LLM for accurate language processing. Consequently, we divide the prompt into language and vision constituents. The first stage of the forward pass processes just the language tokens. In the second stage, these are recombined with the vision represen-

tations within the intermediate layer, before being processed by the latter layers of the LLM. From an implementation point of view, this requires refactoring the LLM’s forward pass as well as the cache structure, so that the model can maintain efficient generation capabilities. Interleaved text and image data poses an additional challenge: Our proposition of splitting and recombining the prompt may lead to inconsistencies with respect to the positional embeddings in the two stages of the forward pass and thus must be accounted for.

Remark: Note that as an alternative, we can pass the same number of dummy multimodal tokens in the first stage (masked out by a suitable attention mask), before replacing them with the vision tokens. Although this approach eases implementation and may help avoid issues with positional embeddings, it naturally reduces the efficiency and empirically leads to worse performance than the alternative.

4.2. Design Considerations

After splitting the prompt, the next question is in which layer the vision tokens should be inserted. If we only cared about efficiency and stronger alignment (Fig. 2), the natural answer would be the last few layers: it would reduce the processing of the tokens in the LLM while potentially leveraging the pre-existing alignment.

However, considering learning capacity militates this choice. Reducing the number of layers through which the vision tokens are processed ultimately lowers the capacity of the LLM to exploit vision information, whether in terms of moving information between vision and language tokens via self-attention or in terms of memory recall within the MLP layers. At present, we sweep this tradeoff by training models with grounding in different layers and comparing their performance. However, finding less computationally expensive proxies for selecting the most appropriate layer via a predefined selection criterion is of interest for future work. Indeed, characterizing the morphospace and associated Pareto frontier for the tradeoff between efficiency and learning capacity, as governed by the architectural choice of grounding layer is an intriguing theoretical question.

5. Experiments

Let us now observe Platonic grounding in action. Our experiments are designed to test grounding in a wide variety of settings: a) for different multimodal frameworks (Vision-language: BLIP, LLaVA) and (Molecular-language: MolCA), b) different base LLM sizes (ranging from 350M to 7B parameter models), and c) LLM architectures (encoder-decoder vs. decoder-only). To account for variations due to training settings (number and type of GPUs, gradient accumulation, etc.), we train the baseline and the grounded ver-

sions for each approach. Our experiments on BLIP follow a custom setup, whereas MolCA and LLaVA are replicated in their predefined setups. In our replication experiments for MolCA and LLaVA, we use the default hyperparameter configurations from the respective repositories for the grounded models, without additional tuning. We report that although LLaVA replicates almost identically, MolCA shows performance gaps with respect to the reported numbers (Liu et al., 2024d). However, the gaps persist for both baseline and grounded versions and therefore do not alter the nature of our conclusions. Finally, note that for brevity, we refer to Platonic grounding as simply *grounding* in the following discussion.

5.1. BLIP

BLIP (Bootstrapped Language-Image Pretraining) is a pioneering approach for vision-language modeling (Li et al., 2022). It introduces a lightweight Querying Transformer (QFormer) that extracts information from the embeddings of the vision encoder. Vision information is transferred into a set of learnable query tokens (32 embeddings of dimension 768) via the QFormer’s cross-attention layers, which are then fed into the LLM along with the language prompt. Further improvements by: a) scaling the LLM and pretraining dataset (Li et al., 2023a), and b) multi-task instruction finetuning (Dai et al., 2023) allows the model to solve a variety of tasks like image captioning, visual question answering, and multimodal reasoning.

In our experiment, we will consider one such model to demonstrate the potential of grounding. Specifically, we consider the VLM’s construction with FlanT5-base (Chung et al., 2022) (encoder-decoder architecture, 350M parameter model) as our LLM and the Eva-clip-g/14 (Sun et al., 2023a), a CLIP-based vision transformer, for our frozen image encoder. The QFormer follows the default architecture and initialization as in Dai et al. (2023). Since FlanT5-base has an encoder-decoder architecture, grounding is performed by bypassing the encoder entirely. Instead of feeding the QFormer outputs (query tokens) as inputs to the encoder, we feed them directly into the decoder by prepending them to the language tokens. The choice of bypassing the encoder is intuitive, since the encoder output space is likely to capture the semantics of the language prompt and therefore align better with the image semantics captured in the QFormer tokens.

Note that we do not intend to follow the training recipe for the InstructBLIP models. Indeed, it is impossible to replicate the model for two reasons: a) lack of information on training recipe, including learning rate schedules and dataset sampling ratios, and b) parts of the LAION dataset, the key component for pretraining, was taken offline so as to comply with U.S. federal law, cf. Thiel (2023). Furthermore,

the high-level recipe calls for multi-epoch pretraining on a dataset with roughly 130M image-text pairs, which are beyond the scope of this work. Instead, we define a smaller setup, which still allows us fair testing of grounding but with a reasonable compute budget. Recall that the end-to-end training phase for InstructBLIP involves two steps: the pretraining step with image-caption pairs, followed by the multi-task instruction finetuning step. Consequently, we structure the experiment in a similar vein.

To emulate InstructBLIP’s training stages, we first pretrain with image-caption pairs for 20 epochs, and then perform multi-task instruction finetuning for captioning and VQA for 15 combined epochs (uniformly sampling from the datasets without replacement). For captioning, we consider the COCO captions dataset as before and for visual question answering, we consider VQAv2 (Goyal et al., 2017) for training. Instruction finetuned VLMs can demonstrate remarkable zero-shot abilities on unseen datasets, and so we also consider OKVQA (Outside Knowledge VQA) (Marino et al., 2019) for zero-shot evaluation. Coco Captions and VQAv2 share the same train-val-test image split that aims to prevent train-test information leakage for a fair evaluation.

Results are given in Table 1. We find that for the designated tasks, our method achieves significant improvements over the standard QFormer. We also see a remarkable gap in zero-shot OKVQA performance, with the grounded model even outperforming the reported performance of some of the largest BLIP-2 models (Li et al., 2023a). (InstructBLIP includes OKVQA during training, so no direct comparison is possible.)

5.2. MolCA

MolCA (Molecular Graph-Language Modeling with Cross-Modal Projector and Uni-Modal Adapter) enables language models to process both molecular graphs and text by bridging the two modalities (Liu et al., 2024d). The training pipeline is almost identical to InstructBLIP: it uses a Cross-Modal Projector (a QFormer with a SciBERT initialization (Beltagy et al., 2019)) to translate information from molecular graph features (obtained from a graph encoder) into learnable query tokens that are fed into the LLM. Additionally, a unimodal low-rank adapter is used to fine-tune the LLM efficiently. The primary tasks considered include molecular-captioning and IUPAC name prediction. To better suit molecular data, Galactica model variants (125M and 1B) are considered as the pretrained LLMs (Taylor et al., 2022).

For our experiments, we follow the exact same training regime as Liu et al. (2024d); the pretraining stage 2 for aligning 2D molecular graphs to texts via language modeling (10 epochs on their curated Pubchem324k pretrain split (Liu et al., 2024d)), followed by finetuning unimodal adapters

| Model | COCO Captions (BLEU-4) | VQAv2 (%) | OKVQA (0-shot) (%) |
|-------------------|------------------------|-------------|--------------------|
| Default (QFormer) | 20.9 | 55.4 | 28.8 |
| Grounded (Ours) | 36.2 | 66.8 | 39.0 |

Table 1. Performance comparison for BLIP-inspired multi-task instruction finetuned models, including 0-shot evaluation on unseen dataset. We find that in our custom setup, bypassing the encoder and grounding directly to the decoder can yield significant performance gains.

for downstream tasks. Since stage 1 does not involve the LLM, we simply start with the Stage 1-pretrained QFormer for both models. We primarily focus on the molecular captioning experiments, using Pubchem324k and CheBI-20 (Edwards et al., 2022). For the LLM, we rely on the larger Galactica-1B variant. Note that since Galactica has a decoder-only architecture with 24 layers, there is no obvious choice of layer for grounding as in the encoder-decoder setting. Thus, we perform grounding for different variants and report their performance in Table 2. For both datasets, we train the model for 100 epochs and check scores every 10 epochs. The performance reported corresponds to the best model performance obtained during the training run. We find that variants of grounding can maintain and even marginally outperform the baseline, while using only half the number of layers for the multimodal tokens.

5.3. LLaVA

LLaVA (Large Language-and-Vision Assistant) is an end-to-end multimodal model that combines a vision encoder with a large language model (LLM), along with a trainable projector MLP that maps visual features onto the LLM embedding space. The model is instruction-tuned in two stages: pretraining for feature alignment and fine-tuning for multimodal conversational tasks. A key innovation is its use of a ChatGPT-generated long-form instruction-following dataset, enabling LLaVA to excel in tasks requiring deep visual comprehension and reasoning.

Given its immense popularity, LLaVA represents a natural testbed for evaluating grounding at scale. For ease of visualization, we will split our experiments into two parts: the first deals solely with performance of different variants, while the second documents the efficiency-performance trade-offs involved in both training and inference.

We evaluate our method with LLaVA v1.5 (Liu et al., 2024a) serving as our baseline on a collection of benchmarks employed by LLaVA v1.5 (Liu et al., 2024a). For a more detailed discussion of these benchmarks, along with their respective evaluation setups and metrics, please refer to Liu et al. (2024a). These benchmarks include GQA (Hudson & Manning, 2019), TextVQA (Singh et al., 2019), SciQA-IMG-IMG (Lu et al., 2022), MME (Xu et al., 2025), POPE (Li et al., 2023b), MMBench (Liu et al., 2024c), and MM-

Vet (Yu et al., 2023). Additionally, we incorporate two more benchmarks with accuracy as the evaluation metric: AI2D (Kembhavi et al., 2016) assessing a model’s ability to comprehend and interpret visual information within diagrams, and MMMU (Yue et al., 2024) evaluating a model’s capability to perceive and integrate multimodal information while applying subject-specific knowledge and reasoning to derive solutions.

5.3.1. PERFORMANCE

For our experiments, we test the application of grounding to the LLaVA-v1.5-7B variant (Liu et al., 2024a). As stated before, this model uses clip-vit-large-patch14-336 (Radford et al., 2021) for the vision encoder, and the decoder-only LLM vicuna-v1.5-7b model (Zheng et al., 2023) with 32 layers. Like MolCA, we perform grounding in different layers and report their performance on key vision language benchmarks in Table 3. Training was performed on 2 NVIDIA A100-80GB GPUs, which took about ~ 60 hours per model for the two stages.

Our results reveal the potential of grounding at scale. Specifically, the variant with grounding in layer 4 manages to remain competitive with the baseline LLaVA model in most baselines, while only utilizing $\frac{7}{8}$ of the total LLM layers for visual token processing. However, we notice that as we attempt grounding in deeper layers, we start to lose competitiveness. This is in line with our analysis in 3, wherein we observed strong visual activity starting in layer 7, which is likely hindered by grounding in latter layers.

Remark It is important to stress that unlike the baseline LLaVA model which has likely been tuned heavily, we did not tune any hyperparameters for any of the grounding variants. Therefore, with an appropriate level of tuning, we strongly believe that grounded models can surpass the baseline in both performance and efficiency, by exploiting the platonic alignment.

5.3.2. PERFORMANCE-EFFICIENCY TRADEOFF

Next, we quantify the efficiency gains for the grounded variants to concretely document the tradeoffs against performance, when applying grounding to LLaVA. We do this in both aspects of training and inference. For training, we use throughput as well as memory utilization for each vari-

| #Insertion Layer | BLEU-2 | BLEU-4 | ROUGE-1 | ROUGE-2 | ROUGE-L | METEOR |
|------------------|-------------|-------------|-------------|-------------|-------------|-------------|
| 0 (Baseline) | 58.3 | <u>49.5</u> | 66.1 | 51.4 | 59.9 | <u>61.3</u> |
| 9 (Grounding) | 58.6 | 49.8 | 66.4 | 51.7 | 60.3 | 61.6 |
| 12 (Grounding) | 58.2 | <u>49.5</u> | <u>66.2</u> | <u>51.6</u> | <u>60.1</u> | <u>61.3</u> |

(a) Molecular Captioning performance on the CheBI-20 dataset for Galactica-1.3B based MolCA models.

| #Insertion Layer | BLEU-2 | BLEU-4 | ROUGE-1 | ROUGE-2 | ROUGE-L | METEOR |
|------------------|-------------|-------------|-------------|-------------|-------------|-------------|
| 0 (Baseline) | 34.1 | 26.4 | 48.5 | 33.9 | 43.1 | 41.8 |
| 9 (Grounding) | <u>34.8</u> | <u>27.2</u> | <u>49.4</u> | <u>34.7</u> | <u>43.8</u> | <u>43.0</u> |
| 12 (Grounding) | 35.3 | 27.7 | 49.7 | 35.3 | 44.3 | 43.4 |

(b) Molecular Captioning performance on the Pubchem324k dataset for Galactica-1.3B based MolCA models.

Table 2. Performances (%) of molecule captioning on the PubChem324k and CheBI-20 datasets. Bold indicates the best performance and underline indicates the second-best performance. The LoRA configurations for finetuning on PubChem324k and CheBI-20 datasets are different, following Liu et al. (2024d). Our results reveal an inherent redundancy with regards to multimodal processing in MolCA: with grounding, we achieve similar or better performance than the baseline, using roughly only half the the LLM for multimodal processing.

| #Insertion Layer | GQA | TextVQA | SciQA-IMG | MME | POPE | MMBench | MM-Vet | AI2D | MMMU |
|------------------|-------------|-------------|-------------|---------------|-------------|-------------|-------------|-------------|-------------|
| 0 (Baseline) | 63.1 | 57.6 | 69.4 | 1436.2 | 86.0 | 66.1 | <u>31.3</u> | 56.2 | <u>36.1</u> |
| 4 (Grounding) | 63.1 | <u>57.5</u> | 68.7 | 1483.9 | 86.0 | <u>66.0</u> | 32.6 | <u>56.0</u> | 36.3 |
| 8 (Grounding) | <u>62.3</u> | 57.1 | <u>68.8</u> | <u>1455.5</u> | <u>84.8</u> | 65.3 | 28.8 | 52.9 | 34.9 |
| 12 (Grounding) | 61.1 | 55.3 | 65.9 | 1248.5 | 83.9 | 55.2 | 30.3 | 52.2 | 35.6 |

Table 3. Performance on various vision-language datasets. Bold indicates the best performance and underline indicates the second-best performance. Our results indicate inherent redundancy in multimodal processing within LLaVA: by incorporating grounding, we can achieve performance comparable to or even surpassing that of the baseline model.

ant, for the finetuning stage. For inference, since different variants may produce different length responses leading to discrepancies in forward pass counts, we proceed in the same manner as the attention visualization experiment; we fix a set of image-text pairs (one image of 576 tokens per prompt of length 88) and track the respective memory utilization as the model processes the inputs.

The results in Table 4 indicate, as expected, that efficiency gains increase for variants with grounding in latter layers. The gains are more for training than inference, but that is down to inference amounting to a single forward pass as per our setup. In practice, we expect a larger inference performance improvement since each call to the generate function involves multiple forward passes. The same holds true for when the number of multimodal tokens are increased. The key takeaway is that grounding (at layer 4) allows us to train a model with the ideal tradeoff: significant efficiency gains while maintaining competitive performance to the baseline.

In addition, the comparison of the instruction tuning training loss plot (Figure 7) shows that platonic grounding models (here again, layer 4) can even achieve a lower final training

loss, indicating the possibility of both a more accurate (in terms of next token prediction) and a more efficient training process.

6. Discussion and Future Work

In this work, we introduced the notion of *Platonic grounding*. Using insights from alignment and interpretability literatures, we provide a natural motivation for the framework. We then back it up with concrete experiments for different VLMs, showcasing improvements in both efficiency and/or performance. Our findings open up several lines of research.

The next step in advancing multimodal grounding is to test its empirical limits, particularly regarding scalability in model size and dataset diversity, as well as for others modalities like speech and video, where long-form content imposes significant computational costs. Additionally, understanding the tradeoff between efficiency (using fewer layers) and performance is key to coming up with a reliable proxy for selecting optimal grounding layers without extensive training is an important direction. Perhaps tools from mechanistic interpretability could help in developing effi-

| #Insertion Layer | #samples/sec | Speedup(%) |
|------------------|--------------|------------|
| 0 (Baseline) | 4.07 | 0% |
| 4 (Grounding) | 4.40 | 8.4% |
| 8 (Grounding) | 4.65 | 14.5% |
| 12 (Grounding) | 5.02 | 23.6% |

(a) Gains in throughput for LLaVA-v1.5-7B model during Stage-2 finetuning.

| #Insertion Layer | Memory Util. (GB) | Reduction(%) |
|------------------|-------------------|--------------|
| 0 (Baseline) | 1.41 | 0% |
| 4 (Grounding) | 0.93 | 34.0% |
| 8 (Grounding) | 0.88 | 37.6% |
| 12 (Grounding) | 0.84 | 40.4% |

(b) Memory gains during inference with batch size=1, estimated by subtracting the memory requirement for loading the base model into memory.

Table 4. Herein, we detail the efficiency gains achieved by different variants of grounding. The key takeaway is that there exists a natural trade-off as we push for efficiency; as can be noted from Table 3, efficiency beyond a certain point (i.e. for layers > 4) come at the cost of performance.

cient ways to predict grounding effectiveness. This will not only provide practical benefits in terms of combining pre-trained models into larger systems, but also help understand the mechanisms of transformer multimodal processing.

7. Impact Statement

Since our work focuses on (pretrained) VLMs, we suffer from the pitfalls associated with such models, including hallucination, equitable access, lack of accountability, and data attribution. At the same time, our proposed method enhances efficiency, potentially lowering computational costs and energy requirements for multimodal model development while maintaining performance, leading to positive societal, economic, and environmental impacts.

References

Alayrac, J.-B., Donahue, J., Luc, P., Miech, A., Barr, I., Hasson, Y., Lenc, K., Mensch, A., Millican, K., Reynolds, M., Ring, R., Rutherford, E., Cabi, S., Han, T., Gong, Z., Samangooei, S., Monteiro, M., Menick, J., Borgeaud, S., Brock, A., Nematzadeh, A., Sharifzadeh, S., Binkowski, M., Barreira, R., Vinyals, O., Zisserman, A., and Simonyan, K. Flamingo: a visual language model for few-shot learning, 2022.

Barsalou, L. W. Grounded cognition: Past, present, and

future. *Topics in Cognitive Science*, 2(4):716–724, 2010.

Basu, S., Grayson, M., Morrison, C., Nushi, B., Feizi, S., and Massiceti, D. Understanding information storage and transfer in multi-modal large language models. arXiv 2406.04236 [cs.CV], 2024.

Beltagy, I., Lo, K., and Cohan, A. SciBERT: A pretrained language model for scientific text. arXiv 1903.10676 [cs.CL], 2019.

Brown, T. B., Mann, B., Ryder, N., Subbiah, M., Kaplan, J., Dhariwal, P., Neelakantan, A., Shyam, P., Sastry, G., Askell, A., Agarwal, S., Herbert-Voss, A., Krueger, G., Henighan, T., Child, R., Ramesh, A., Ziegler, D. M., Wu, J., Winter, C., Hesse, C., Chen, M., Sigler, E., Litwin, M., Gray, S., Chess, B., Clark, J., Berner, C., McCandlish, S., Radford, A., Sutskever, I., and Amodei, D. Language models are few-shot learners. arXiv 2005.14165 [cs.CL], 2020.

Buccino, G., Colagè, I., Gobbi, N., and Bonaccorso, G. Grounding meaning in experience: A broad perspective on embodied language. *Neuroscience & Biobehavioral Reviews*, 69:69–78, 2016.

Caron, M., Touvron, H., Misra, I., Jégou, H., Mairal, J., Bojanowski, P., and Joulin, A. Emerging properties in self-supervised vision transformers. arXiv 2104.14294 [cs.CV], 2021.

Chung, H. W., Hou, L., Longpre, S., Zoph, B., Tay, Y., Fedus, W., Li, Y., Wang, X., Dehghani, M., Brahma, S., Webson, A., Gu, S. S., Dai, Z., Suzgun, M., Chen, X., Chowdhery, A., Castro-Ros, A., Pellat, M., Robinson, K., Valter, D., Narang, S., Mishra, G., Yu, A., Zhao, V., Huang, Y., Dai, A., Yu, H., Petrov, S., Chi, E. H., Dean, J., Devlin, J., Roberts, A., Zhou, D., Le, Q. V., and Wei, J. Scaling instruction-finetuned language models. arXiv 2210.11416 [cs.LG], 2022.

Dai, W., Li, J., Li, D., Tiong, A. M. H., Zhao, J., Wang, W., Li, B., Fung, P., and Hoi, S. InstructBLIP: Towards general-purpose vision-language models with instruction tuning. arXiv 2305.06500 [cs.CV], 2023.

Dettmers, T., Pagnoni, A., Holtzman, A., and Zettlemoyer, L. QLoRA: Efficient finetuning of quantized LLMs. arXiv 2305.14314 [cs.LG], 2023.

Edwards, C., Lai, T., Ros, K., Honke, G., Cho, K., and Ji, H. Translation between molecules and natural language. arXiv 2204.11817 [cs.CL], 2022.

Fang, Z., Wang, J., Hu, X., Wang, L., Yang, Y., and Liu, Z. Compressing visual-linguistic model via knowledge distillation. arXiv 2104.02096 [cs.CV], 2021.

- Goyal, Y., Khot, T., Summers-Stay, D., Batra, D., and Parikh, D. Making the v in vqa matter: Elevating the role of image understanding in visual question answering, 2017.
- Grattafiori, A., Dubey, A., Jauhri, A., Pandey, A., Kadian, A., Al-Dahle, A., Letman, A., Mathur, A., Schelten, A., Vaughan, A., Yang, A., Fan, A., and et al. The llama 3 herd of models, 2024. URL <https://arxiv.org/abs/2407.21783>.
- Hendel, R., Geva, M., and Globerson, A. In-context learning creates task vectors, 2023. URL <https://arxiv.org/abs/2310.15916>.
- Hoffmann, J., Borgeaud, S., Mensch, A., Buchatskaya, E., Cai, T., Rutherford, E., de Las Casas, D., Hendricks, L. A., Welbl, J., Clark, A., Hennigan, T., Noland, E., Millican, K., van den Driessche, G., Damoc, B., Guy, A., Osindero, S., Simonyan, K., Elsen, E., Rae, J. W., Vinyals, O., and Sifre, L. Training compute-optimal large language models, 2022. URL <https://arxiv.org/abs/2203.15556>.
- Hu, E. J., Shen, Y., Wallis, P., Allen-Zhu, Z., Li, Y., Wang, S., Wang, L., and Chen, W. Lora: Low-rank adaptation of large language models, 2021a. URL <https://arxiv.org/abs/2106.09685>.
- Hu, E. J., Shen, Y., Wallis, P., Allen-Zhu, Z., Li, Y., Wang, S., Wang, L., and Chen, W. Lora: Low-rank adaptation of large language models, 2021b. URL <https://arxiv.org/abs/2106.09685>.
- Hudson, D. A. and Manning, C. D. Gqa: A new dataset for real-world visual reasoning and compositional question answering. In *Proceedings of the IEEE/CVF conference on computer vision and pattern recognition*, pp. 6700–6709, 2019.
- Huh, M., Cheung, B., Wang, T., and Isola, P. The platonic representation hypothesis. *arXiv preprint arXiv:2405.07987*, 2024.
- Jiang, Z., Chen, J., Zhu, B., Luo, T., Shen, Y., and Yang, X. Devils in middle layers of large vision-language models: Interpreting, detecting and mitigating object hallucinations via attention lens, 2025. URL <https://arxiv.org/abs/2411.16724>.
- Kaplan, J., McCandlish, S., Henighan, T., Brown, T. B., Chess, B., Child, R., Gray, S., Radford, A., Wu, J., and Amodei, D. Scaling laws for neural language models. *CoRR*, abs/2001.08361, 2020. URL <https://arxiv.org/abs/2001.08361>.
- Kembhavi, A., Salvato, M., Kolve, E., Seo, M., Hajishirzi, H., and Farhadi, A. A diagram is worth a dozen images. In *Computer Vision—ECCV 2016: 14th European Conference, Amsterdam, The Netherlands, October 11–14, 2016, Proceedings, Part IV 14*, pp. 235–251. Springer, 2016.
- Kriegeskorte, N. and Kievit, R. A. Representational geometry: integrating cognition, computation, and the brain. *Trends in Cognitive Sciences*, 17(8):401–412, August 2013.
- Lenc, K. and Vedaldi, A. Understanding image representations by measuring their equivariance and equivalence, 2015. URL <https://arxiv.org/abs/1411.5908>.
- Leviathan, Y., Kalman, M., and Matias, Y. Fast inference from transformers via speculative decoding, 2023. URL <https://arxiv.org/abs/2211.17192>.
- Li, J., Li, D., Xiong, C., and Hoi, S. Blip: Bootstrapping language-image pre-training for unified vision-language understanding and generation, 2022.
- Li, J., Li, D., Savarese, S., and Hoi, S. Blip-2: Bootstrapping language-image pre-training with frozen image encoders and large language models, 2023a.
- Li, Y., Du, Y., Zhou, K., Wang, J., Zhao, W. X., and Wen, J.-R. Evaluating object hallucination in large vision-language models. *arXiv preprint arXiv:2305.10355*, 2023b.
- Liu, H., Li, C., Li, Y., and Lee, Y. J. Improved baselines with visual instruction tuning. In *Proceedings of the IEEE/CVF Conference on Computer Vision and Pattern Recognition*, pp. 26296–26306, 2024a.
- Liu, H., Li, C., Wu, Q., and Lee, Y. J. Visual instruction tuning. *Advances in neural information processing systems*, 36, 2024b.
- Liu, Y., Duan, H., Zhang, Y., Li, B., Zhang, S., Zhao, W., Yuan, Y., Wang, J., He, C., Liu, Z., et al. Mmbench: Is your multi-modal model an all-around player? In *European conference on computer vision*, pp. 216–233. Springer, 2024c.
- Liu, Z., Li, S., Luo, Y., Fei, H., Cao, Y., Kawaguchi, K., Wang, X., and Chua, T.-S. Molca: Molecular graph-language modeling with cross-modal projector and uni-modal adapter, 2024d. URL <https://arxiv.org/abs/2310.12798>.
- Locke, J. *An Essay Concerning Human Understanding*. Thomas Bassett, London, 1690.

- Lu, P., Mishra, S., Xia, T., Qiu, L., Chang, K.-W., Zhu, S.-C., Tafjord, O., Clark, P., and Kalyan, A. Learn to explain: Multimodal reasoning via thought chains for science question answering. *Advances in Neural Information Processing Systems*, 35:2507–2521, 2022.
- Lv, A., Chen, Y., Zhang, K., Wang, Y., Liu, L., Wen, J.-R., Xie, J., and Yan, R. Interpreting key mechanisms of factual recall in transformer-based language models. arXiv 2403.19521 [cs.CL], 2024.
- Marino, K., Rastegari, M., Farhadi, A., and Mottaghi, R. OK-VQA: A visual question answering benchmark requiring external knowledge. arXiv 1906.00067 [cs.CV], 2019.
- Merullo, J., Eickhoff, C., and Pavlick, E. A mechanism for solving relational tasks in transformer language models, 2024. URL <https://openreview.net/forum?id=ZmzLrl8nTa>.
- Moschella, L., Maiorca, V., Fumero, M., Norelli, A., Locatello, F., and Rodolà, E. Relative representations enable zero-shot latent space communication. arXiv 2209.15430 [cs.LG], 2023.
- Mountcastle, V. B. The columnar organization of the neocortex. *Brain*, 120:701–722, 1997.
- OpenAI, Achiam, J., Adler, S., Agarwal, S., Ahmad, L., Akkaya, I., et al. GPT-4 technical report. arXiv 2303.08774 [cs.CL], 2024.
- Ouyang, L., Wu, J., Jiang, X., Almeida, D., Wainwright, C. L., Mishkin, P., Zhang, C., Agarwal, S., Slama, K., Ray, A., Schulman, J., Hilton, J., Kelton, F., Miller, L., Simens, M., Askell, A., Welinder, P., Christiano, P., Leike, J., and Lowe, R. Training language models to follow instructions with human feedback. arXiv 2203.02155 [cs.CL], 2022.
- Putnam, H. Three kinds of scientific realism. *The Philosophical Quarterly*, 32(128):195–200, 1982.
- Qi, Y., Li, H., Song, Y., Wu, X., and Luo, J. How vision-language tasks benefit from large pre-trained models: A survey. arXiv 2412.08158 [cs.CV], 2024.
- Radford, A., Kim, J. W., Hallacy, C., Ramesh, A., Goh, G., Agarwal, S., Sastry, G., Askell, A., Mishkin, P., Clark, J., Krueger, G., and Sutskever, I. Learning transferable visual models from natural language supervision. arXiv 2103.00020 [cs.CV], 2021.
- Singh, A., Natarajan, V., Shah, M., Jiang, Y., Chen, X., Batra, D., Parikh, D., and Rohrbach, M. Towards VQA models that can read. In *Proceedings of the IEEE/CVF Conference on Computer Vision and Pattern Recognition*, pp. 8317–8326, 2019.
- Srinivasan, K., Raman, K., Chen, J., Bendersky, M., and Najork, M. WIT: Wikipedia-based image text dataset for multimodal multilingual machine learning. In *Proceedings of the 44th International ACM SIGIR Conference on Research and Development in Information Retrieval*, pp. 2443–2449, 2021.
- Strubell, E., Ganesh, A., and McCallum, A. Energy and policy considerations for deep learning in NLP. arXiv 1906.02243 [cs.CL], 2019.
- Sun, Q., Fang, Y., Wu, L., Wang, X., and Cao, Y. EVA-CLIP: Improved training techniques for CLIP at scale. arXiv 2303.15389 [cs.CV], 2023a.
- Sun, Z., Shen, S., Cao, S., Liu, H., Li, C., Shen, Y., Gan, C., Gui, L.-Y., Wang, Y.-X., Yang, Y., Keutzer, K., and Darrell, T. Aligning large multimodal models with factually augmented RLHF. arXiv 2309.14525 [cs.CV], 2023b.
- Taylor, R., Kardas, M., Cucurull, G., Scialom, T., Hartshorn, A., Saravia, E., Poulton, A., Kerkez, V., and Stojnic, R. Galactica: A large language model for science. arXiv 2211.09085 [cs.CL], 2022.
- Thiel, D. Identifying and Eliminating CSAM in Generative ML Training Data and Models. *Stanford Internet Observatory*, 2023.
- Tian, Y., Krishnan, D., and Isola, P. Contrastive multiview coding. arXiv 1906.05849 [cs.CV], 2020.
- Touvron, H., Martin, L., Stone, K., Albert, P., Almahairi, A., et al. Llama 2: Open foundation and fine-tuned chat models. arXiv 2307.09288 [cs.CL], 2023.
- Wang, T., Zhou, W., Zeng, Y., and Zhang, X. EfficientVLM: Fast and accurate vision-language models via knowledge distillation and modal-adaptive pruning. arXiv 2210.07795 [cs.CL], 2022.
- Wang, X., Chen, J., Wang, Z., Zhou, Y., Zhou, Y., Yao, H., Zhou, T., Goldstein, T., Bhatia, P., Huang, F., and Xiao, C. Enhancing visual-language modality alignment in large vision language models via self-improvement. arXiv 2405.15973 [cs.CV], 2024.
- Xu, P., Shao, W., Zhang, K., Gao, P., Liu, S., Lei, M., Meng, F., Huang, S., Qiao, Y., and Luo, P. LVLm-EHub: A comprehensive evaluation benchmark for large vision-language models. *IEEE Transactions on Pattern Analysis and Machine Intelligence*, 47(3):1877–1893, 2025.
- Yu, W., Yang, Z., Li, L., Wang, J., Lin, K., Liu, Z., Wang, X., and Wang, L. MM-Vet: Evaluating large multimodal models for integrated capabilities. arXiv 2308.02490 [cs.AI], 2023.

Yue, X., Ni, Y., Zhang, K., Zheng, T., Liu, R., , et al. MMMU: A massive multi-discipline multimodal understanding and reasoning benchmark for expert AGI. In *Proceedings of the IEEE/CVF Conference on Computer Vision and Pattern Recognition*, pp. 9556–9567, 2024.

Zhai, X., Kolesnikov, A., Houlsby, N., and Beyer, L. Scaling vision transformers. arXiv 2106.04560 [cs.CV], 2021.

Zheng, L., Chiang, W.-L., Sheng, Y., Zhuang, S., Wu, Z., Zhuang, Y., Lin, Z., Li, Z., Li, D., Xing, E. P., Zhang, H., Gonzalez, J. E., and Stoica, I. Judging LLM-as-a-Judge with MT-Bench and Chatbot Arena. arXiv 2306.05685 [cs.CL], 2023.

Zimmermann, R. S., Sharma, Y., Schneider, S., Bethge, M., and Brendel, W. Contrastive learning inverts the data generating process. arXiv 2102.08850 [cs.LG], 2022.

A. Alignment in DINO

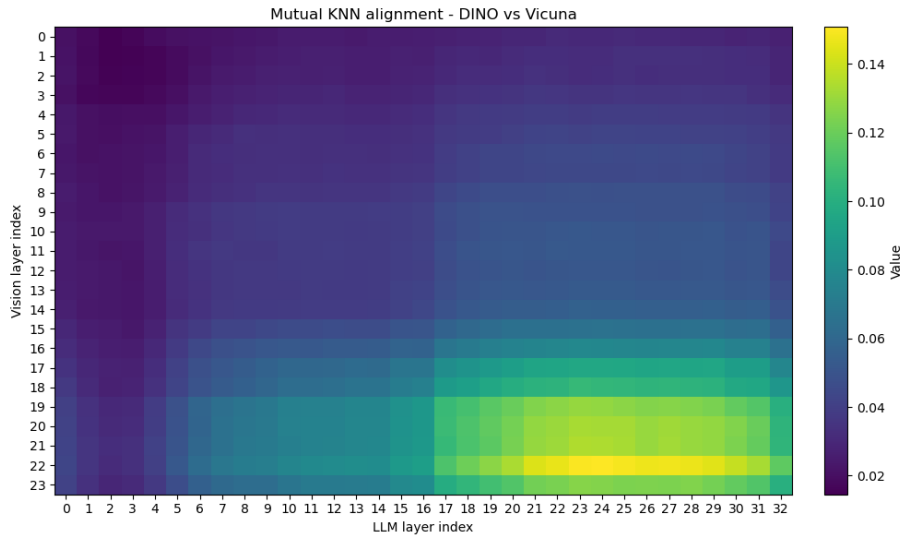


Figure 5. Visualization of intrinsic alignment between pretrained vision (DINO-based ViT) and language models (Vicuna v1.5), as a function of depth. The trend is similar to that for CLIP-based models, in for the representations from the latter vision layers (generally used as embeddings), alignment becomes stronger as one moves deeper into the LLM.

B. Where Visual Tokens Matter

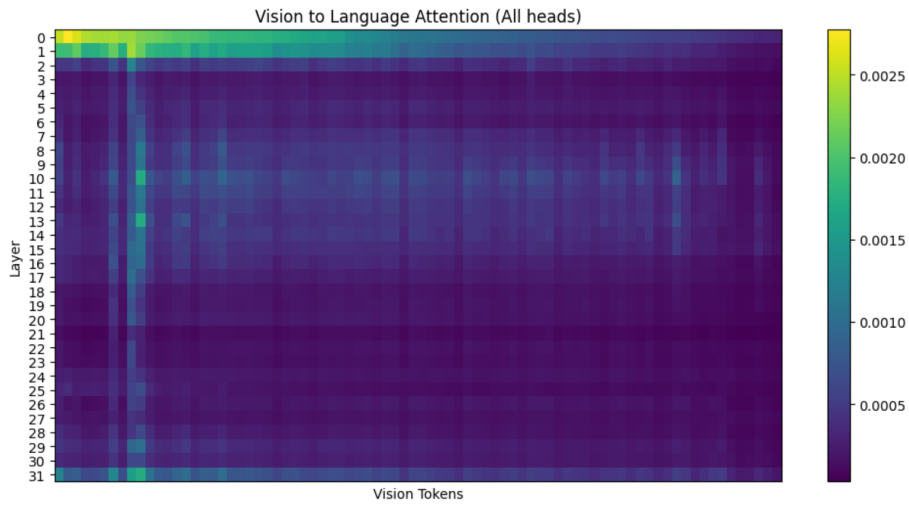


Figure 6. Full illustration of vision to language token activations (including the first two layers), in the forward pass of a LLaVA-v1.5-7B model. The vertical axis represents the LLM layer indices and the horizontal axis consists of vision tokens in the forward pass, arranged left-to-right in increasing positional indices. The legend represents the strength attention activity.

C. Training Loss Comparison on LLaVA

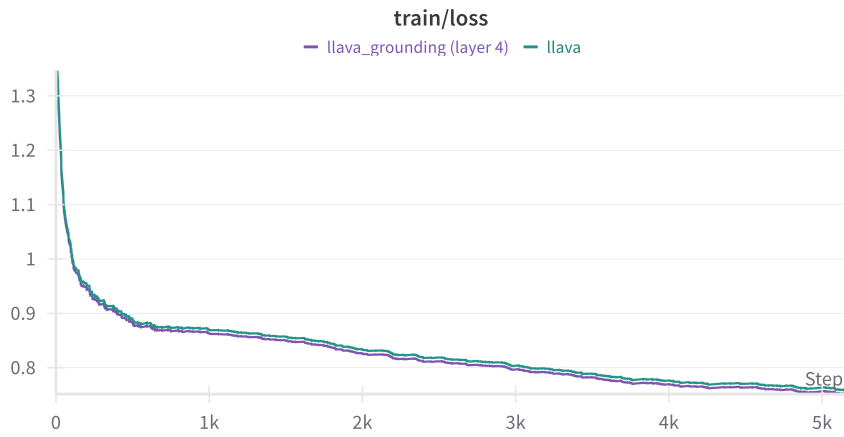


Figure 7. Comparison of training losses of LLaVA finetuning stage, for the baseline model against best performing grounded model (layer-4), revealing a tendency to achieve lower next token prediction loss and potentially better learning.